HHS Public Access

Author manuscript

Int J Biol Macromol. Author manuscript; available in PMC 2021 June 15.

Published in final edited form as:

Int J Biol Macromol. 2020 June 15; 153: 100–106. doi:10.1016/j.ijbiomac.2020.02.253.

Small Ultra-Red Fluorescent Protein Nanoparticles as Exogenous Probes for Noninvasive Tumor Imaging *In Vivo*

Feifei An[a,b], **Nandi Chen**[b,c], **William J. Conlon**[d], **Justin S. Hachey**[d], **Jingqi Xin**[a], **Omer Aras**[e], **Erik A. Rodriguez**[d,*], **Richard Ting**[b,*]

[a]Institute of Medical Engineering, Department of Biophysics, School of Basic Medical Science, Health Science Center, Xi'an Jiaotong University, No.76 Yanta West Road, Xi'an, Shaanxi, 710061, P. R. China.

[b]Department of Radiology, Weill Cornell Medicine, New York, NY 10065, USA.

[c]Department of Gastrointestinal Surgery, The Second Clinical Medicine College (Shenzhen People's Hospital) of Jinan University, Shenzhen, Guangdong 518020, China.

[d]Department of Chemistry, The George Washington University, Washington, DC 20052, USA.

[e]Department of Radiology, Memorial Sloan Kettering Cancer Center, New York, NY, 10065, USA.

Abstract

Nanoparticles are excellent imaging agents for cancer, but variability in chemical structure, racemic mixtures, and addition of heavy metals hinders FDA approval in the United States. We developed a small ultra-red fluorescent protein, named smURFP, to have optical properties similar to the small-molecule Cy5, a heptamethine subclass of cyanine dyes (Ex/Em = 642/670 nm). smURFP has a fluorescence quantum yield of 18% and expresses so well in *E. coli*, that gram quantities of fluorescent protein are purified from cultures in the laboratory. In this research, the fluorescent protein smURFP was combined with bovine serum albumin into fluorescent protein nanoparticles. These nanoparticles are fluorescent with a quantum yield of 17% and 12–14 nm in diameter. The far-red fluorescent protein nanoparticles noninvasively image tumors in living mice via the enhanced permeation and retention (EPR) mechanism. This manuscript describes the use of a new fluorescent protein nanoparticle for *in vivo* fluorescent imaging. This protein nanoparticle core should prove useful as a biomacromolecular scaffold, which could bear extended chemical modifications for studies, such as the *in vivo* imaging of fluorescent protein nanoparticles targeted

*Corresponding Authors.: erik_rodriguez@gwu.edu (E. A. Rodriguez); rct2001@med.cornell.edu (R. Ting).

AUTHOR STATEMENT

Feifei An, Erik A. Rodriguez, and Richard Ting designed experiments and wrote the manuscript. Feifei An and Nandi Chen synthesized nanoparticles and performed *in vitro* and *in vivo* experiments. Jingqi Xin collected absorbance and fluorescence data and images. William J. Conlon and Justin S. Hachey purified the small ultra-red fluorescent protein and synthesized nanoparticles. Feifei An, Omer Aras, Erik A. Rodriguez, and Richard Ting analyzed and discussed the data.

Declaration of competing interest

The authors declare that there is no conflict of interest.

Appendix A. Supplementary Data

Supplementary data for this article is available online.

to primary and metastatic cancer, theranostic treatment, and/or dual-modality imaging with positron emission tomography for entire human imaging.

Keywords

Far-red fluorescence; Fluorescent protein; Protein nanoparticle; Cancer imaging; Tumor imaging

1. Introduction

Fluorescence probes are essential for biological imaging and allow for human cancer cell and tumor imaging.[1, 2] Fluorescence is becoming the imaging modality of choice for live cell imaging at subcellular resolution and in multiplex imaging, or imaging multiple targets simultaneously with different color fluorescence. These technologies are proving useful for the preoperative diagnosis of cancer and in intraoperative, fluorescence guided surgery.[3–5] Many fluorescent probes exist for tumor imaging *in vivo*, including small molecule dyes, fluorescent proteins, quantum dots, fluorescent polymers, upconversion nanoparticles, and labelled biological macromolecules, such as antibodies.[6–9]

Fluorescent proteins (FPs) are widely used in biomedical research applications for genetically labeling endogenous proteins or adding biosensors for visualizing proteins, small molecules, enzyme activity, and ions inside cells.[10] The original green fluorescent protein is excited by ~480 nm and fluoresces at ~510 nm. While useful *in vitro*, these wavelengths of light are limited *in vivo*, because of limited through-tissue penetration (<0.5 mm) due to absorbance, scattering, reflection, and autofluorescence by endogenous molecules. Deep tissue photon penetration is needed for true utility in *in vivo* clinical diagnosis and fluorescence guided surgery. New fluorescent proteins, like the small ultra-red fluorescent protein (smURFP), exhibit far-red and near-infrared fluorescence (650–900 nm) and is preferred for noninvasive fluorescence imaging *in vivo* due to deeper light penetration through biological tissue.[11]

Unfortunately, the transgenic encoding of fluorescent proteins into living human tissue is not currently a feasible strategy for identifying endogenous cancer, which would require incorporation of the transgene into cancer cells and not normal cells. The use of ***free*** fluorescent protein is an alternative strategy, but single dispersed proteins, like bovine serum albumin (~4 nm), are too small to accumulate at the tumor preferentially by passive targeting *via* the Enhanced Permeation and Retention (EPR) mechanism.[14,15] Nanoparticles are excellent scaffolds for passive cancer imaging *in vivo*, unfortunately, the chemical synthesis of dendrimers and polymers often result in an impure mixture of chemical structures, different molecular weight species, and racemates. Heavy metal nanoparticles and quantum dots contain heavy metals that can induce off-target toxicity to nearby healthy tissue. Protein nanoparticles or biological macromolecules are excellent alternatives that are translated by the ribosome as a single enantiomer into pure-molecular weight structures, but require further modification with an exogenous small molecule dye to fluorescently image. New probes are necessary for developing far-red and near-infrared fluorescent probes that lack chemical modification for fluorescent imaging, retained in the blood for a significant period

of time for passive tumor targeting through enhanced permeation and retention (EPR), and are amenable to chemical modification for cancer targeting, treatment, and multi-modality imaging.[12]

We developed a small ultra-red fluorescent protein, named smURFP, with spectral characteristics similar to the heptamethine cyanine dye, Cy5 (Ex/Em = 642/670 nm), from a cyanobacterial phycobiliprotein. smURFP has a fluorescence quantum yield of 18%, extinction coefficient of 180,000 M^{-1} cm^{-1}, and expresses extremely well in *E. coli* for safe isolation at gram quantities of fluorescent protein.[13] Expression quantity, far-red fluorescence, and biophysical brightness (quantum yield X extinction coefficient) make smURFP an excellent choice for tumor imaging *in vivo*. To force smURFP to intrinsically accumulate at the tumor via the EPR effect, we transformed smURFP into a nanoparticle with serum albumin. In previous work, we found that bovine serum albumin aggregates form nanoparticles that accumulate at the tumor *via* passive EPR targeting, while ***free*** serum albumin does not accumulate at tumors *in vivo*. [14, 15] This research inspired us to pack the fluorescent protein, smURFP, with our bovine serum albumin to create fluorescent protein nanoparticles that are fluorescent, without external chemical modification.

The far-red fluorescent protein, smURFP, was combined with bovine serum albumin in an oil and water emulsion to synthesize fluorescent protein nanoparticles. The fluorescent protein nanoparticles remain fluorescent, with a quantum yield of 17% and fluorescence emission at 667 nm. The fluorescent nanoparticles are stable in the bloodstream after intravenous injection and allow for noninvasive passive tumor imaging in mice. The fluorescent protein nanoparticles show no apparent toxicity *in vitro* and *in vivo* by MTT assay for cell metabolic activity and H&E histology of major organs, respectively. The fluorescent protein nanoparticles are excellent biomacromolecule scaffolds for further modification for targeting primary and metastatic cancer for *in vivo* theranostics and/or multi-modality positron emission tomography (PET) or magnetic resonance imaging (MRI) for imaging in entire humans.

2. Materials and Methods

2.1. Materials and instruments

smURFP was purified from *E. coli* expressing HO-1 for biliverdin production by Ni-NTA column as previously described.[13] Bovine serum albumin (BSA) and dichloromethane (DCM) were purchased from Sigma-Aldrich (USA). A549 cell lines were purchased from American Type Culture Collection (ATCC CCL-185). BALB/c nude mice were purchased from Charles River Laboratories (USA). The animal work was approved by the Weill Cornell Medical Center Institutional Animal Care and Use Committee (#2014–0030, mice) and are consistent with the recommendations of the American Veterinary Medical Association, the National Institutes of Health Guide for the Care and Use of Laboratory Animals, and the ARRIVE guidelines.

Transmission electronic microscope (TEM) images of fluorescent protein nanoparticles were obtained with a TEM (JEM-1400, JEOL, Tokyo, Japan) at a voltage of 120 kV. The hydrodynamic size of the prepared fluorescent protein nanoparticles were measured by

dynamic light scattering (Malvern Zetasizer Nano-S). Absorbance and fluorescence spectra of the prepared fluorescent protein nanoparticles were obtained by Cary 60 UV-Vis Spectrophotometer and Cary Eclipse Fluorescence Spectrometer (Agilent Technologies, Santa Clara, CA, USA), respectively. Eppendorf tube and animal fluorescence were imaged with an *In Vivo* Xtreme Imaging System (Bruker, Billerica, MA).

2.2. Methods

2.2.1. Preparation of the fluorescent protein nanoparticles—An 0.18 mL quantity of isolated smURFP protein (20 mM, 1x PBS, pH 7.4) was combined with 3 mL BSA (6 mg/mL, 1x PBS, pH 7.4). 0.8 mL DCM was added to the protein in PBS and sonicated to form an emulsion. DCM was removed by overnight stirring and slow evaporation. The protein and PBS solution were centrifuged at 8,000 rpm for 10 min to remove bulk aggregate. The supernatant, which contains the desired fluorescent protein nanoparticles, was collected for fluorescence imaging experiments. The prepared fluorescent protein nanoparticles were characterized with dynamic light scattering (DLS) at 25 °C to determine size. For TEM size characterization, the nanoparticles were added to a copper grid and stained with 0.5% uranyl acetate for 1 min.

2.2.2. Photophysical properties—The absorbance spectra of fluorescent protein nanoparticles in 1x PBS, pH 7.4 was measured with a Cary 60 UV-Vis Spectrophotometer. The fluorescence emission spectra of the fluorescent protein nanoparticles in 1x PBS, pH 7.4 was measured with a Cary Eclipse Fluorescence Spectrometer with excitation of 580 nm.

Fluorescence images were obtained with a Bruker *In Vivo* Xtreme Imaging System. A 1 μM solution of fluorescent protein nanoparticles (1x PBS, pH 7.4) in an Eppendorf tube was excited at 630 nm and fluorescence emissions were collected with a 700 nm long pass filter.

2.2.3. Fluorescence stability of fluorescent protein nanoparticles at various pH—The nanoparticles were incubated in different pH phosphate buffers for 24 h. Nanoparticle fluorescence was measured at different pH using a 620 nm excitation light source. Fluorescent emission intensities were collected at different pH values. A Bruker *In Vivo* Xtreme Imaging System was used to image fluorescent nanoparticles.

2.2.4. Fluorescent protein nanoparticle hydrodynamic diameter stability measurements—Dynamic light scattering diameter measurements of fluorescent protein nanoparticles were obtained in 1x PBS buffer (pH 7.4) every 24 h for 168 h (7 d).

2.2.5. Biocompatibility of the fluorescent protein nanoparticle—A549 cancer cells (ATCC) were seeded in 96-well plate at a density of 4,000 cells/well. After 24 h, the fluorescent protein nanoparticles were added to the cells and incubated for 24 h at 37 °C. A549 cell incubations, without nanoparticles were used as the control group. Cytoviability was evaluated with a standard 3-(4,5-dimethylthiazol-2-yl)-2,5-diphenyltetrazolium bromide (MTT) colorimetric assay. The absorbance at 490 nm was measured and normalized to the control group. All fluorescent protein nanoparticle concentration groups were measured in triplicate.

2.2.6. Cell imaging with the fluorescent protein nanoparticles—A549 cancer cells were seeded in 24-well plate and cultured for 24 h at 37 °C. The cells were incubated with 1 μM fluorescent protein nanoparticles and after 24 h, the cells were washed three times with 1x PBS, pH 7.4 and stained with DAPI. The cells were imaged with EVOS fluorescence microscope (Life Technologies) with a Cy5 LED cube (Ex/Em: 628(40)/ 692(40) nm).

2.2.7. Noninvasive fluorescence imaging of A549 tumor xenograft *in vivo*— BALB/c nude mice were implanted with subcutaneous A549 flank tumors. The tumors were imaged when they grew to ~150 mm^3. A 200 μL solution of fluorescent protein nanoparticles in 1x PBS (pH 7.4) was intravenously injected via tail vein. Mice were imaged with a Bruker *In Vivo* Xtreme Imaging System before the injection, 2, 4, 6, 12, and 24 h post injection. Mice were imaged using 630 nm excitation light and a and a 700 nm long pass filter. Free far-red fluorescent protein, smURFP, was intravenously injected via tail vein and imaged as a control group.

2.2.8. Calculation of biodistribution via. *ex vivo* fluorescence imaging— Xenograft bearing BALB/c nude mice were sacrificed 24 h after being intravenously injected with fluorescent protein nanoparticles. Organs were collected and imaged with a Bruker *In Vivo* Xtreme Imaging System. Organs were imaged using 630 nm excitation light and a 700 nm long pass filter. The mean fluorescence intensities of each organ from three mice for each condition were measured and plot for comparison. The mice of the group injected with free far-red fluorescent protein, smURFP, was set as a control.

3. Results and Discussions

To prepare fluorescent protein nanoparticles, small ultra-red fluorescent protein (smURFP) and bovine serum albumin were dissolved together in 1x PBS (pH 7.4). Dichloromethane (DCM) was added and the mixture was sonicated to form an oil in water (o/w) emulsion. The o/w system was stirred overnight in an uncapped flask. DCM was then removed by slow evaporation (Figure 1a). To confirm the successful loading of small ultra-red fluorescent protein (smURFP) into the fluorescent protein nanoparticles, the solution was centrifuged. A blue color was observed in both the solution and precipitate in the Eppendorf tube (Figure 1b, inset). The observed blue color in the precipitate confirms emulsion-method-formation of smURFP aggregates and the pellet was discarded. Only the supernatant was used for fluorescence imaging experiments. Dynamic light scattering (DLS) was used to measure BSA protein with a ~4 nm diameter. The ***free*** smURFP absorbs the DLS laser line and did not allow accurate DLS measurements of the pure protein (Figure 1b).[13] DLS imaging of the fluorescent protein nanoparticles show a diameter of ~14 nm, indicating the formation of an aggregate of several BSA and smURFP proteins. TEM images of fluorescent protein nanoparticle showed an average size of ~12 nm, which is similar to the DLS measurement of ~14 nm and most likely caused by shrinkage while the particles dried on the copper grid (Figure 1c).

Fluorescent protein nanoparticles exhibit maximum absorbance and fluorescence emission at 644 and 666 nm, respectively (Figure 2a). ***Free*** smURFP has a maximum absorbance and

fluorescence pass filter for deep tissue penetration and noninvasive imaging (Figure 2b).[16] The absorbance and fluorescence spectra of the fluorescent protein nanoparticles are similar to the ***free*** small ultra-red fluorescent protein (smURFP). The quantum yield of the fluorescent protein nanoparticles was measured using methylene blue in ethanol as a reference standard (QY = 4%).[17] Fluorescent protein nanoparticles have a 17% quantum yield of fluorescence, which is slightly lower and within error of smURFP (18%).[13] These results demonstrate that the fluorescent protein maintains its tertiary structure around the chromophore. Unfolded smURFP protein would result in significant loss in fluorescence intensity and quantum yield reduction. At the measured level of incorporation into the nanoparticles, smURFP does not show significant homo Förster Resonance Energy Transfer (FRET). This suggests that one fluorescent protein with one fluorescent chromophore is incorporated per nanoparticle. Two fluorescent chromophores reduce the quantum yield by homo FRET.[13] If there was significant FRET, the quantum yield of the fluorescent protein nanoparticle would be less than 17%. An unperturbed fluorescence intensity and quantum yield of the chromophore within the fluorescent protein nanoparticle is essential for noninvasive fluorescence imaging *in vivo*.

In an alternative synthesis, we failed to combine the small ultra-red fluorescent protein (smURFP) and serum albumin by the reprecipitation method of nanoparticle synthesis. Ethanol was gradually added to the mixture of protein to force protein aggregation due to decreased solubility. Nanoparticles formed by the reprecipitation method were not fluorescent, suggesting that the this method unfolds smURFP allowing the chromophore to become flexible, solvent exposed, and no longer fluorescent (data not shown). The emulsion method (Figure 1a) is preferred for preparing fluorescent protein nanoparticles for fluorescent imaging applications.

The internal pH inside a cell depends on the subcellular compartment being measured and ranges from 4.5–8.0 depending on the organelle. Most fluorescent proteins are not stable in acidic environments, such as the lysosomes and endosomes, as indicated by a diminished fluorescence intensity. ***Free*** smURFP has a $pK_a = 3.2$. We tested if the pK_a was altered in the fluorescent protein nanoparticle core. The fluorescence of the nanoparticle was determined at various pH values. Fluorescent protein nanoparticles show stable fluorescence intensity between pH 4.5–8.0 with no significant change (Figure 3). These results demonstrate that the fluorescence of fluorescent protein nanoparticles are resistant to changes in pH between 4.5–8.0. This range allows fluorescent protein nanoparticles to be suitable for pH measurements in all organelles within the cell, including in acidic lysosomes and endosomes, and the acidic environment of tumors *in vivo*.

Fluorescent protein nanoparticle stability was studied by measuring its diameter over time by dynamic light scattering (DLS). The diameter of solutions of fluorescent protein nanoparticles in 1x PBS, pH 7.4 was measured by DLS every 24 h for 7 days. The average measured fluorescent protein nanoparticle diameter varied between 12–15 nm, which is typical of DLS measurements (Figure 4). These DLS measurements indicate that fluorescent protein nanoparticle diameters are stable for days in 1x PBS at room temperature. Room temperature stability is important for predicting clinical translatability because room temperature storage is preferred and more readily accessible. The diameter size of 12–15 nm

and stable diameter of the nanoparticles facilitates accumulation via the enhanced permeation and retention (EPR) effect in tumors within the optimum range of 10–200 nm. [18] Research showed 12–15 nm diameter nanoparticles are reliably delivered to poorly permeable tumors *in vivo*.[19] Therefore, we tested our 12–15 nm diameter fluorescent protein nanoparticles for imaging poorly permeable tumors *in vivo*.

Before *in vivo* studies, we measured if the fluorescent protein nanoparticles are non-toxic to cells. Lung cancer (A549) cells were incubated with fluorescent protein nanoparticles at different concentrations for 24 h. The viability of A549 cells was evaluated in standard MTT assays. The MTT assays indicates no change in cytoviability at concentrations ≤50 μM after 24 h exposure (Figure 5). The MTT assays showed the fluorescent protein nanoparticles are not cytotoxic to A549 lung cancer cells *in vitro*.

We tested if fluorescent protein nanoparticles could enter cells passively. Fluorescent protein nanoparticles were incubated with A549 cells for 24 h. Fluorescent microcopy showed the fluorescent protein nanoparticles entered A549 cells by non-specific endocytosis. After vigorous washing, three times with 1x PBS, red fluorescence was visible inside cells, suggesting non-specific uptake of fluorescent protein nanoparticles by A549 cells. Endocytosed fluorescent protein nanoparticles show stable fluorescence for at least 24 h at 37 °C. These results confirm that the fluorescent protein nanoparticles are stable, even following endocytosis.

Fluorescent protein nanoparticles were used to noninvasively image A549 tumor xenografts *in vivo*. A baseline, background image of BALB/c mice bearing an A549 tumor xenograft was collected before injection of fluorescent protein nanoparticles (Figure 7 Left). Mice (n = 3) were imaged at 2, 4, 6, 12, and 24 h following intravenous fluorescent protein nanoparticle injection. Fluorescence contrast in the tumor that is above background is clearly visible 2 h after contrast injection (Figure 7, Red Arrow). 24 h post injection, the tumor maintains its fluorescence intensity suggesting that the fluorescent protein nanoparticles are stable *in vivo*. The fluorescence signal in neighboring, non-tumor tissue decreases steadily as excess circulating nanoparticles are removed from circulation. The reduced background signal enhances the signal to background contrast (Figure 7). In contrast, the ***free*** small ultra-red fluorescent protein, smURFP, does exhibit efficient tumor accumulation and imaging post *i.v.* injection (Figure S2). The small, 2–3 nm diameter of smURFP shows rapid clearance from the blood and does not accumulate in tumors by the EPR effect. Fluorescent protein nanoparticles are useful for noninvasively imaging tumors *in vivo* 2–24 h post injection because the fluorescent protein nanoparticles accumulate in tumors by the EPR effect.

After *in vivo* imaging (Figure 7), mice were sacrificed, and organs were harvested. Organs were imaged with a Bruker *In Vivo* Xtreme Imaging System with 630 nm excitation and 700 nm long pass filter (Figure 8a). The fluorescence intensities of the *ex vivo* organs from three mice were averaged (Figure 8b). Tumor fluorescence has the largest signal, followed by clearance organs, including liver, spleen, and lung. *Ex vivo* organ imaging demonstrates that the probe is primarily removed by the hepatic system (liver), lung, and spleen. The renal system (kidney) does not appear to remove the fluorescent protein nanoparticles. The

injected fluorescent protein nanoparticles are retained at the tumor site 24 h post administration and was removed by specific clearance organs, which clearly demonstrates the value of fluorescence imaging to confirm nanoparticle biodistribution temporally in living mice (Figure 7) and after death in organs (Figure 8). Tumor fluorescent signal is greatest 24 h post administration (Figure 8b). In contrast, the fluorescence distribution of the ***free*** small ultra-red fluorescent protein, smURFP, is mainly at the stomach and low at the tumor (Figure S3). The results correspond to the non-invasive mice imaging lacking ***free*** smURFP accumulation in the tumor by EPR (Figure S2). H&E histology sections of the collected organs show no obvious side effect of the synthesized nanoparticles (Figure S4).

4. Conclusions

We describe a method for synthesizing stable fluorescent protein nanoparticles containing a novel, small ultra-red fluorescent protein (smURFP). This fluorescent protein is an optimal choice because the protein fluoresces in the far-red and near-infrared, is biophysically bright, stable at acidic pH, and large quantities are isolated from *E. coli*. The biophysical brightness, acid stability of the fluorescent chromophore, and fluorescence in the far-red allows this fluorescent protein nanoparticle to be visualized deeper through tissue. Fluorescent protein nanoparticles retain a similar quantum yield to ***free*** smURFP, which suggests that a single, folded smURFP is incorporated per nanoparticle. Increased incorporation of smURFP would result in diminished quantum yield by homo Förster Resonance Energy Transfer (FRET) and red-shifted fluorescence, which is seen with two chromophores.[13] Unfolded protein would result in a decrease in absorbance, fluorescence, and quantum yield caused by chromophore exposure to solvent and increased flexibility of the chromophore.

The fluorescent protein nanoparticles retain fluorescence stability across a range of pH (4.5–8.0) (Figure 3). The diameter of the fluorescent protein nanoparticles is ~12–15 nm and remains constant following 7 days of incubation in 1x PBS, pH 7.4 at room temperature (Figure 4). No visible toxicity was seen in MTT assays (Figure 5), fluorescence imaging with A549 cells (Figure 6), and in mouse organs after 24 h (Figure S4).

Fluorescent protein nanoparticles were used to noninvasively imaged A549 tumor xenografts *in vivo* via the EPR effect (Figure 7). Specific tumor fluorescence signal is visible 2 – 24 h post-injection, where the greatest fluorescence signal-to-noise signal is visible 24 h post injection. Fluorescent protein nanoparticles are cleared from the circulation of mice through the liver, spleen, and lung. Probe accumulation is not observed in the kidneys of mice. This study shows that fluorescent protein nanoparticles could be useful for imaging solid tumors in the kidney and other organs with low background fluorescence. The ***free*** smURFP injected into mice showed no accumulation in the tumor after 24 h (Figure S2) and clearance was through the stomach (Figure S3). Clearly, size matters and the fluorescent protein nanoparticles at 12–14 nm are preferred for imaging tumors in vivo relative to the ***free*** smURFP.

We describe a new fluorescent protein nanoparticle scaffold. This smURFP containing, fluorescent protein nanoparticle is useful for fluorescent imaging. Chemical modification of the fluorescent protein nanoparticles extends utility of this fluorescent biomacromolecular

scaffold to allow targeted *in vivo* imaging of cancer, theranostic treatment, nanoparticle drug delivery, and/or dual-modality imaging with positron emission tomography for whole body imaging.

Supplementary Material

Refer to Web version on PubMed Central for supplementary material.

Acknowledgements

This work was supported by the GW Cancer Center and Katzen Research Cancer Research Pilot Award to E. A. Rodriguez.

References

[1]. Gao M, Yu FB, Lv CJ, Choo J, Chen LX, Fluorescent chemical probes for accurate tumor diagnosis and targeting therapy, Chem. Soc. Rev 46(8) (2017) 2237–2271. [PubMed: 28319221]

[2]. Liu JN, Bu WB, Shi JL, Chemical Design and Synthesis of Functionalized Probes for Imaging and Treating Tumor Hypoxia, Chem. Rev 117(9) (2017) 6160–6224. [PubMed: 28426202]

[3]. Wang CS, Wang ZH, Zhao T, Li Y, Huang G, Sumer BD, Gao JM, Optical molecular imaging for tumor detection and image-guided surgery, Biomaterials 157 (2018) 62–75. [PubMed: 29245052]

[4]. Sun Y, Ding MM, Zeng XD, Xiao YL, Wu HP, Zhou H, Ding BB, Qu CR, Hou W, Er-bu AGA, Zhang YJ, Cheng Z, Hong XC, Novel bright-emission small-molecule NIR-II fluorophores for in vivo tumor imaging and image-guided surgery, Chem. Sci 8(5) (2017) 3489–3493. [PubMed: 28507722]

[5]. Ni X, Zhang XY, Duan XC, Zheng HL, Xue XS, Ding D, Near-Infrared Afterglow Luminescent Aggregation-Induced Emission Dots with Ultrahigh Tumor-to-Liver Signal Ratio for Promoted Image-Guided Cancer Surgery, Nano Lett. 19(1) (2019) 318–330. [PubMed: 30556699]

[6]. Yan F, Wu H, Liu HM, Deng ZT, Liu H, Duan WL, Liu X, Zheng HR, Molecular imaging-guided photothermal/photodynamic therapy against tumor by iRGD-modified indocyanine green nanoparticles, J. Control. Release 224 (2016) 217–228. [PubMed: 26739551]

[7]. Lv GX, Guo WS, Zhang W, Zhang TB, Li SY, Chen SZ, Eltahan AS, Wang DL, Wang YQ, Zhang JC, Wang PC, Chang J, Liang XJ, Near-Infrared Emission CuInS/ZnS Quantum Dots: All-in-One Theranostic Nanomedicines with Intrinsic Fluorescence/Photoacoustic Imaging for Tumor Phototherapy, ACS Nano 10(10) (2016) 9637–9645. [PubMed: 27623101]

[8]. Sheng ZH, Guo B, Hu DH, Xu SD, Wu WB, Liew WH, Yao K, Jiang JY, Liu CB, Zheng HR, Liu B, Bright Aggregation-Induced-Emission Dots for Targeted Synergetic NIR-II Fluorescence and NIR-I Photoacoustic Imaging of Orthotopic Brain Tumors, Adv. Mater 30(29) (2018) 1800766.

[9]. Chan MH, Pan YT, Chan YC, Hsiao M, Chen CH, Sun LD, Liu RS, Nanobubble-embedded inorganic 808 nm excited upconversion nanocomposites for tumor multiple imaging and treatment, Chem. Sci 9(12) (2018) 3141–3151. [PubMed: 29732096]

[10]. Rodriguez EA, Campbell RE, Lin JY, Lin MZ, Miyawaki A, Palmer AE, Shu XK, Zhang J, Tsien RY, The Growing and Glowing Toolbox of Fluorescent and Photoactive Proteins, Trends Biochem. Sci 42(2) (2017) 111–129. [PubMed: 27814948]

[11]. Guo ZQ, Park S, Yoon J, Shin I, Recent progress in the development of near-infrared fluorescent probes for bioimaging applications, Chem. Soc. Rev 43(1) (2014) 16–29. [PubMed: 24052190]

[12]. Shu X, Royant A, Lin MZ, Aguilera TA, Lev-Ram V, Steinbach PA, Tsien RY, Mammalian expression of infrared fluorescent proteins engineered from a bacterial phytochrome. Science 324 (2009) 804–807. [PubMed: 19423828]

[13]. Rodriguez EA, Tran GN, Gross LA, Crisp JL, Shu XK, Lin JY, Tsien RY, A far-red fluorescent protein evolved from a cyanobacterial phycobiliprotein, Nat. Methods 13(9) (2016) 763–769. [PubMed: 27479328]

[14]. An FF, Deng ZJ, Ye J, Zhang JF, Yang YL, Li CH, Zheng CJ, Zhang XH, Aggregation-Induced Near-Infrared Absorption of Squaraine Dye in an Albumin Nanocomplex for Photoacoustic Tomography in Vivo, ACS Appl. Mater. Interfaces 6(20) (2014) 17985–17992. [PubMed: 25223319]

[15]. An FF, Yang YL, Liu J, Ye J, Zhang JF, Zhou MJ, Zhang XJ, Zheng CJ, Liang XJ, Zhang XH, A reticuloendothelial system-stealthy dye-albumin nanocomplex as a highly biocompatible and highly luminescent nanoprobe for targeted in vivo tumor imaging, RSC Adv. 4(12) (2014) 6120–6126.

[16]. Zhao P, Xu Q, Tao J, Jin ZW, Pan Y, Yu CM, Yu ZQ, Near infrared quantum dots in biomedical applications: current status and future perspective, Wiley Interdiscip. Rev.-Nanomed. Nanobiotechnol 10(3) (2018) 16.

[17]. Kelly JM, van der Putten WJM, McConnell DJ, Laser flash spectrooscopy of methylene blue with nucleic acids, Photochemistry and Photobiology 45(2) (1987) 167–175. [PubMed: 3562581]

[18]. Ren Z, Sun S, Sun R, Cui G, Hong L, Rao B, Li A, Yu Z Kan Q and Mao Z, A Metal–Polyphenol-Coordinated Nanomedicine for Synergistic Cascade Cancer Chemotherapy and Chemodynamic Therapy, Adv. Mater 36 (2) (2020) 1906024.

[19]. Cabral H, Matsumoto Y, Mizuno K, Chen Q, Murakami M, Kimura M, Terada Y, Kano MR, Miyazono K, Uesaka M, Nishiyama N, Kataoka K, Accumulation of sub-100 nm polymeric micelles in poorly permeable tumours depends on size, Nat. Nanotechnol 6(12) (2011) 815–823. [PubMed: 22020122]

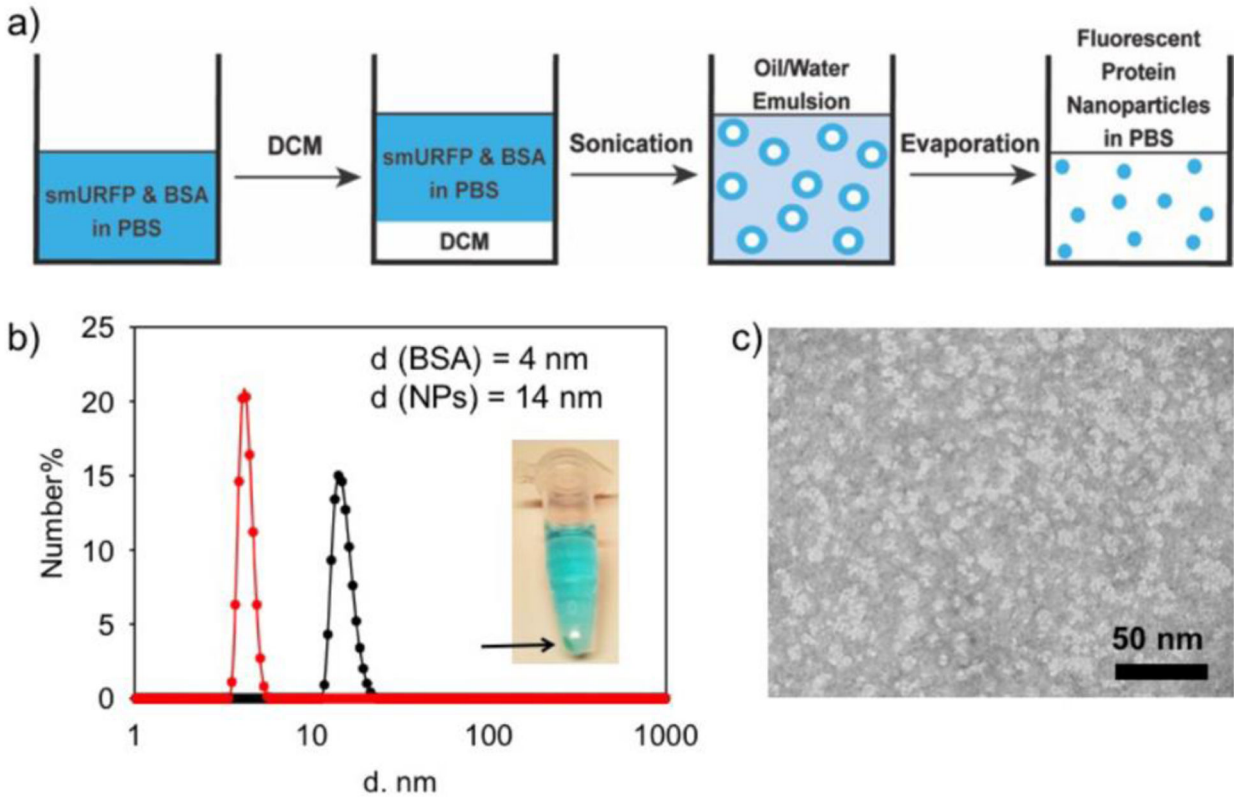

Figure 1.

Synthesis and size characterization of fluorescent protein nanoparticles. a) Schematic of fluorescent protein nanoparticle preparation by the emulsion method. b) The DLS characterization of BSA and the fluorescent protein nanoparticles (NPs). Diameter (d) is shown on the X-axis with a log scale. Inset: Centrifuged Eppendorf tube showing precipitated protein in the pellet and fluorescent protein nanoparticles in solution. c) TEM image of fluorescent protein nanoparticles negatively stained with 0.5% uranyl acetate. Fluorescent protein nanoparticles are shown as white in the image.

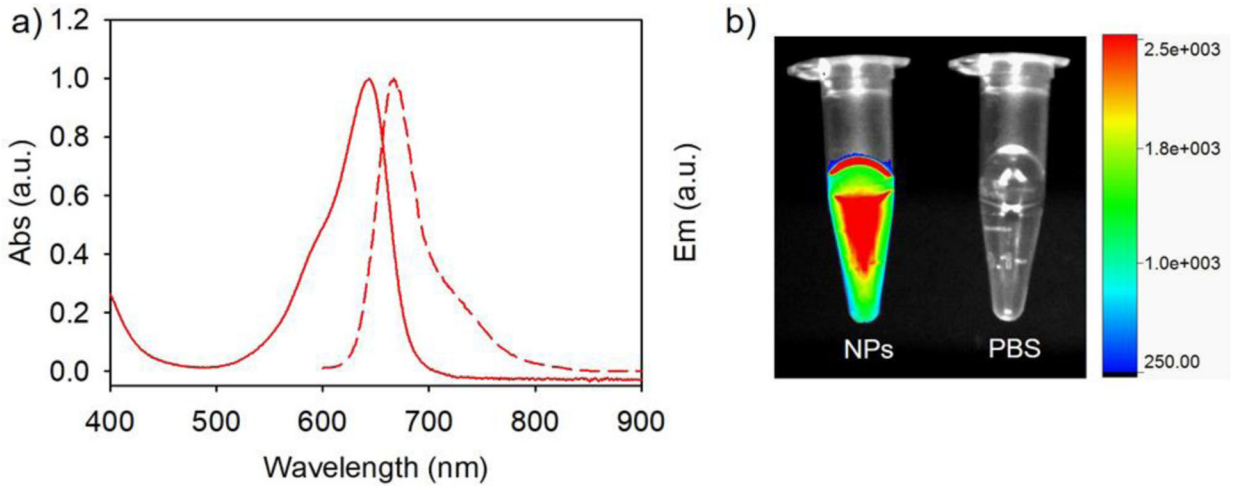

Figure 2.

Biophysical characterization and fluorescence image of fluorescent protein nanoparticles. a) The absorbance and fluorescence emission spectra of fluorescent protein nanoparticles in 1x PBS, pH 7.4. b) Overlay of fluorescence and white light images of fluorescent protein nanoparticles in 1x PBS solution, pH 7.4 (NPs, Left) and 1x PBS, pH 7.4 (Right). Fluorescence imaged with 630 nm excitation and 700 nm long pass filter.

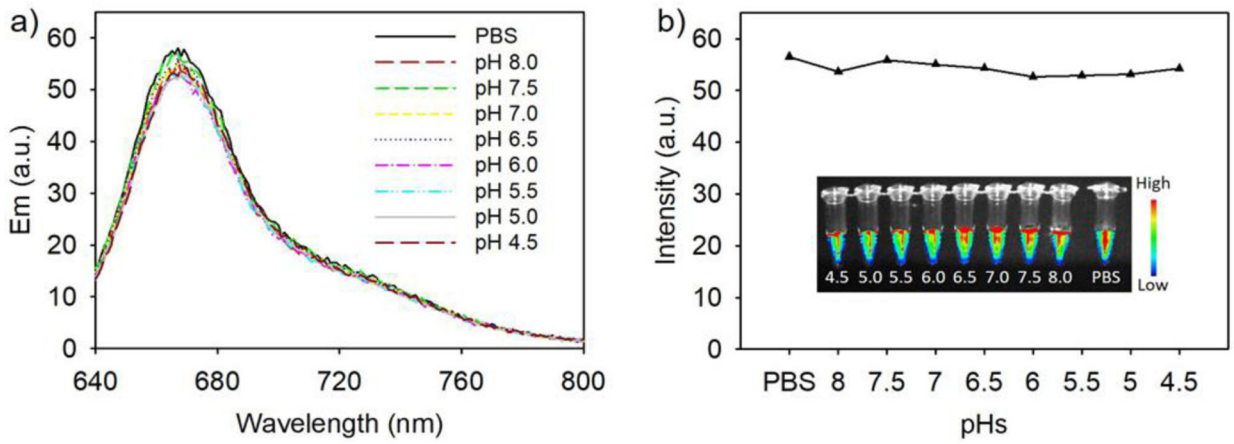

Figure 3.

Fluorescence stability of fluorescent protein nanoparticles at various pH. a) Fluorescence of fluorescent protein nanoparticles at pH 4.5–8.0. ‘PBS’ is pH 7.4. Fluorescence spectra were obtained with excitation at 620 nm. b) Plot of the fluorescence intensities at maximum fluorescence emission. Inset: Fluorescence image of the fluorescent protein nanoparticles at different pH values in Eppendorf tubes. Fluorescence images were obtained with excitation at 630 nm and a 700 nm long pass filter.

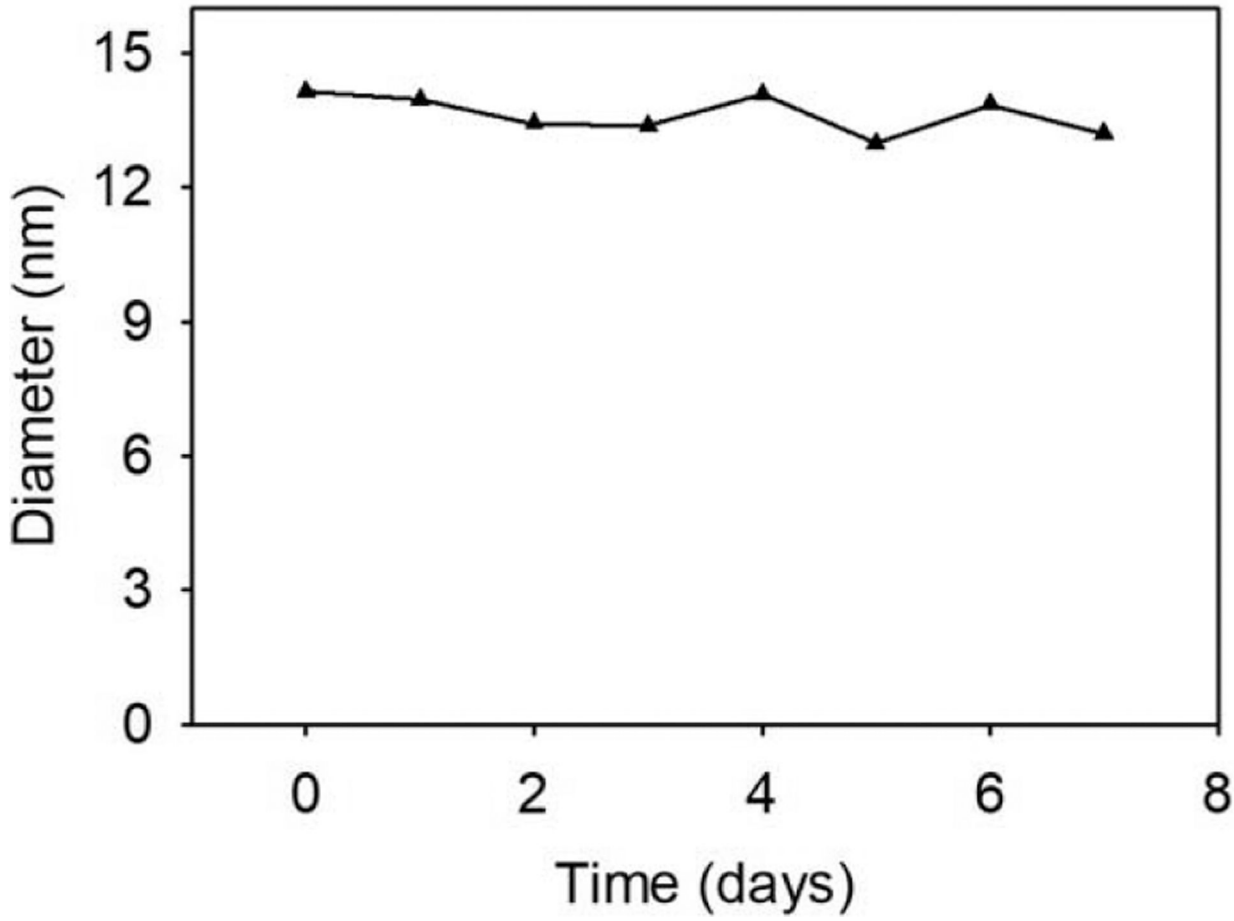

Figure 4.

Measurement of the fluorescent protein nanoparticle diameters as a function of time. The diameters were measured by dynamic light scattering at 25 °C.

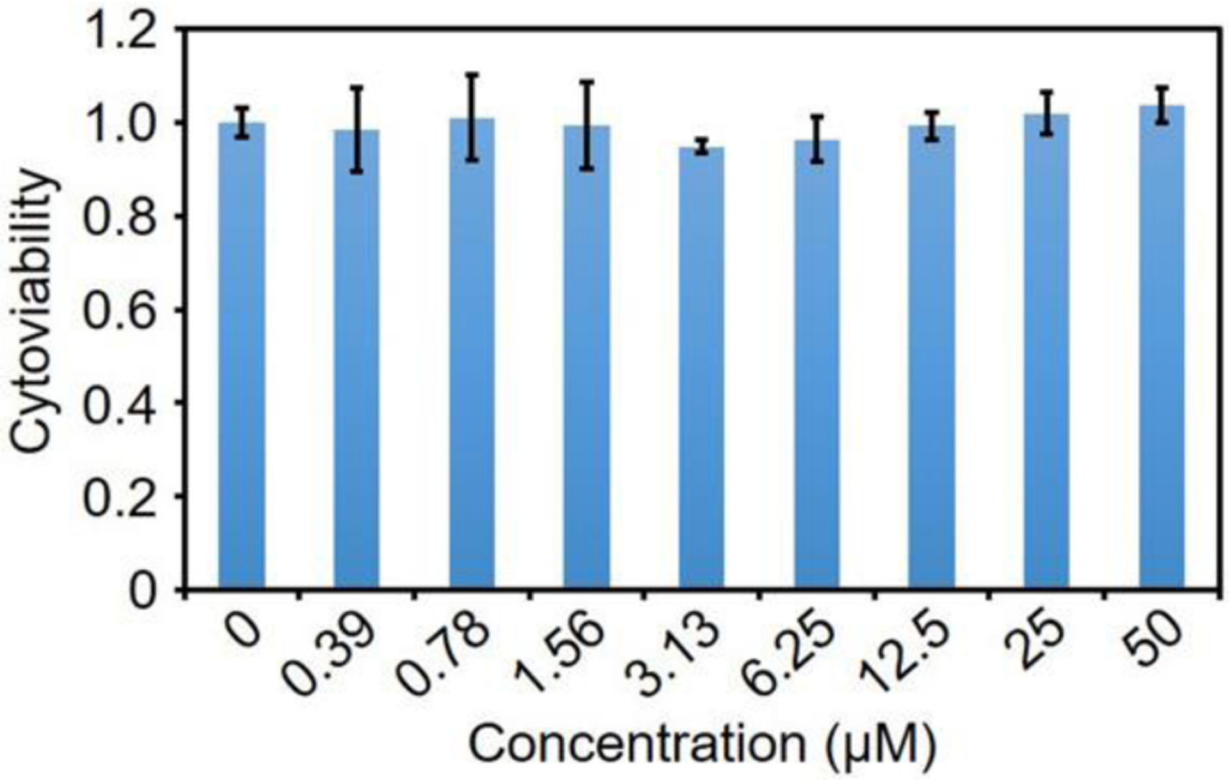

Figure 5.

Viability of A549 cells after incubation with fluorescent protein nanoparticles for 24 h. Concentrations are listed on the X-axis and were repeated in triplicate. Error bars are ± SEM.

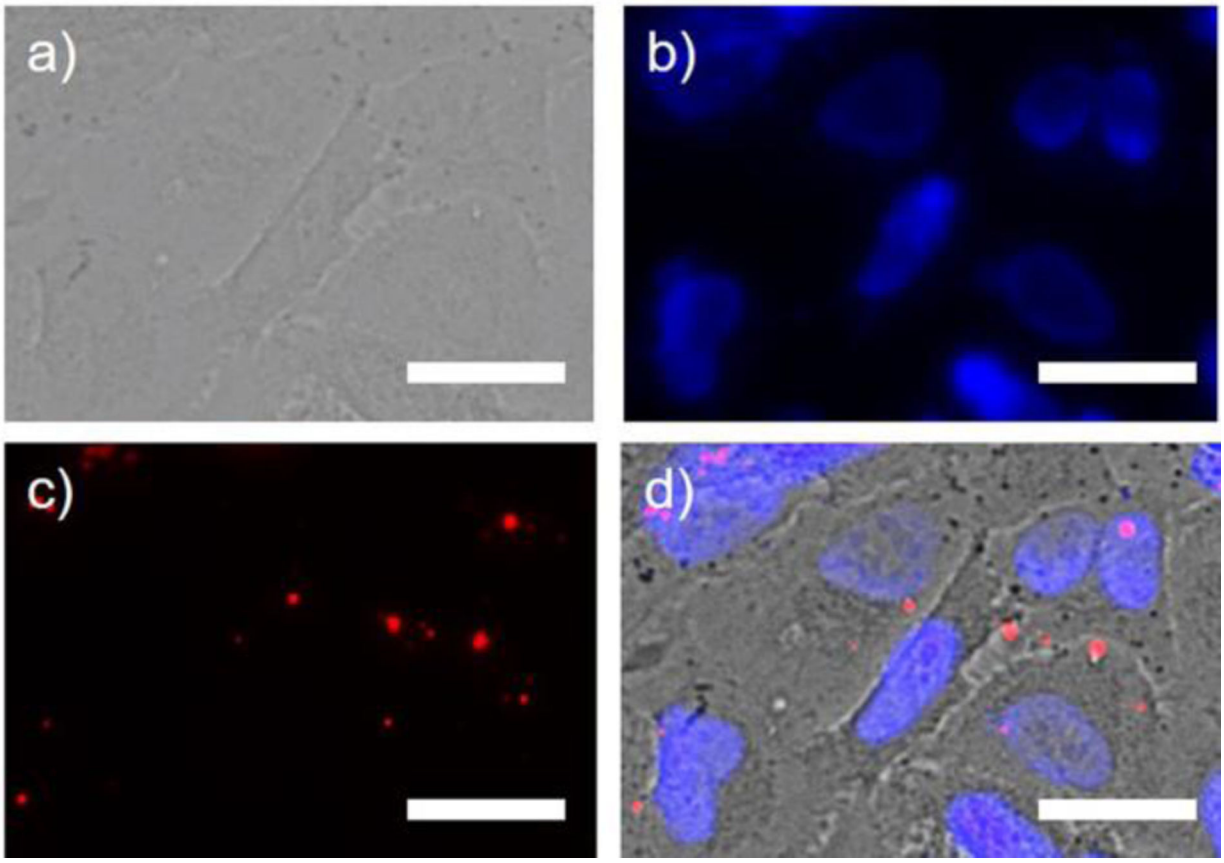

Figure 6.

Images of A549 cancer cells incubated with fluorescent protein nanoparticles. a) Bright-field image of A549 cells. b) A549 cancer cell nuclei stained with DAPI (Blue). c) A549 cancer cells labelled with fluorescent protein nanoparticles (Red). Fluorescence was visible after three washes with 1x PBS. d) Overlay of a), b), and c). Fluorescent protein nanoparticles are not expected to enter the cells without targeting, however, some non-specific nanoparticle endocytosis was observed in endosomes and/or lysosomes. We hypothesize that punctate, distinct fluorescence spots appear larger than ~14 nm due to the diffraction of fluorescence light, but may also be multiple nanoparticles and undiscernible by widefield imaging. Scale bar is 25 μm.

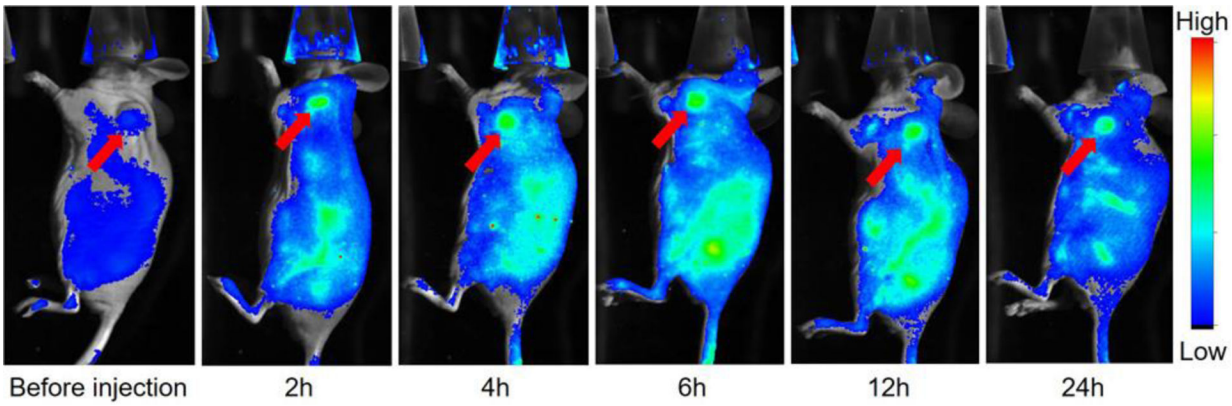

Figure 7.

Fluorescence imaging of fluorescent protein nanoparticles injected intravenously through the tail vein in nude mice with an A549 tumor xenograft (Red Arrow). Representative mouse images before injection and 2, 4, 6, 12, and 24 h after fluorescent protein nanoparticle injection. Images are overlay of fluorescence (Rainbow LUT) and bright field (gray). Fluorescence imaged with *In Vivo* Xtreme Imaging System (Bruker).

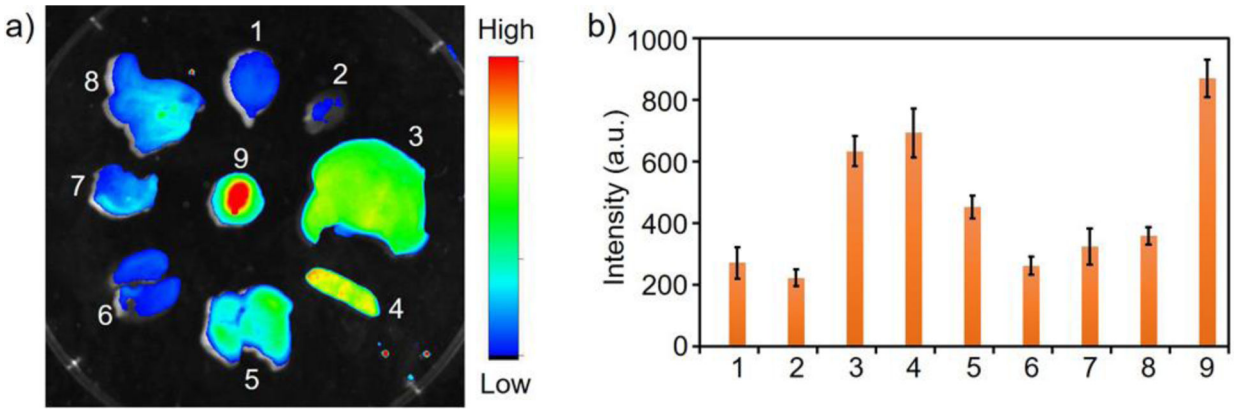

Figure 8.

Biodistribution of fluorescent protein nanoparticles *ex vivo*. a) Representative *ex vivo* fluorescence image of organs 24 h post fluorescent protein nanoparticle injection (*In Vivo* Xtreme Imaging System (Bruker)). b) Biodistribution analysis of nanoparticle in mice (n = 3) by *ex vivo* organ fluorescence. X-axis: 1 - brain, 2 - heart, 3 - liver, 4 - spleen, 5 - lung, 6 - kidney, 7 - stomach, 8 - intestine, and 9 -tumor. Error bars are ± SEM.